ASIAN JOURNAL OF CIVIL ENGINEERING (BUILDING AND HOUSING) VOL. 6, NO. 6 (2005)
PAGES 457-476

SEISMIC EVALUATION AND ECONOMICAL STRENGTHENING OF REINFORCED CONCRETE BUILDINGS

T. Kabeyasawa*
Earthquake Research Institute, The University of Tokyo, Tokyo, Japan

ABSTRACT

Seismic evaluation standard for existing reinforced concrete buildings is outlined which has been in practical use from 1970' in Japan. An effective, efficient and economical method is introduced using polyester sheet for strengthening old and non-ductile buildings. The remarkable effectiveness on the improvement of deformability has been verified through a various seismic tests such as number of static column tests and a shaking table test of frames, and already in practical use for columns. The verification test on walls strengthened with the polyester sheet was conducted recently. Since the conventional detail for strengthening walls with fabric sheets is generally complicated, a new detail for strengthening walls was developed. The bare reinforced concrete wall failed in a brittle shear failure mode, while much higher shear strength and deformability after flexural yielding were observed generally for the walls strengthened with the sheet. The new detail improved the deformability much more than the conventional detail.

Keywords: retrofits, deformability, shear strength, column, wall, fabric sheet

1. INTRODUCTION

Low-rise reinforced concrete buildings in Japan suffered remarkably and unexpected damages occurred associated with brittle shear failure of columns by the 1968 Tokachi-oki Earthquake. This encouraged a variety of research, which resulted in the revision of Enforcement Order of the Building Standard Law of Japan and AIJ Standard for Structural Calculation of Reinforced Concrete Structures in 1971. A drastic revision in practice was on the minimum requirement of column hoop, namely that the minimum ratio was specified as 0.002, and the maximum spacing as 100mm previously 300mm, which ensures deformability of columns to some adequate degree in most cases only with these specifications. Some of old reinforced concrete buildings, especially those built before 1971, collapsed due to the brittle shear failure of columns, during major earthquakes such as 1978 Miyagiken-oki and 1995 Kobe earthquakes. Although about one third of existing buildings at present were built before 1971 and still remains vulnerable as constructed, seismic

* Email-address of the corresponding author: kabe@eri.u-tokyo.ac.jp

evaluation and retrofit of these buildings have progressed very slowly and are still urgently needed to reduce loss-of-life due to major earthquakes.

Seismic evaluation of reinforced concrete buildings in Japan has been based on the "Standard for Seismic Evaluation of Existing Reinforced Concrete Buildings," since mid 1970', published by Japan Building Disaster Prevention Association. The standard has been in practical use and revised every ten years. The only recent 2001 edition [JBPDA, 2001] has become available in English [JBPDA, 2005].

In some cases of these old reinforced concrete buildings under a major earthquake, the columns would lose their gravity-load carrying capacity due to inadequate amount of confining hoops or shear reinforcement causing collapse like so-called pancake. To avoid such unpleasant incident, retrofit of weak members would be necessary. However, the seismic retrofit of an old building is still so expensive that the progress of retrofit is too slow-paced worldwide. Developing an economical way of retrofit for the existing seismic vulnerable buildings is one of the most important technological targets in earthquake engineering.

To make old and brittle reinforced concrete columns ductile economically, a method of retrofit named as SRF (Super Retrofit with Flexibility) using flexible and ductile chemical fabric sheet such as polyester sheet has been developed and verified through seismic tests on columns and frame specimens [Kabeyasawa et al, 2001-2004]. The brittle column could be made super-ductile up to the deformability of 20 percent story drift angle to survive extreme earthquake motions much higher than prescribed in design codes. The method is generally less expensive than the conventional methods and could be much less by dissemination. Also the retrofit using SRF could be made applicable to various members such as walls or other structural systems such as infill frames, masonry, adobe, timber and so on.

On the other hand, strengthening using fabric sheet such carbon and aramid for columns has been applied to reinforced concrete walls. In case of strengthening walls with irregular shape of the horizontal section with boundary columns, complicated details are necessary to anchor the sheet at the edges of the wall panel. In spite of this complication, the performance was not so much improved as in case for strengthening columns because confinement by the sheet was effective only in the boundary columns. A new detail for strengthening walls with polyester sheet was developed using special joint devices. Three wall specimens, a bare reinforced concrete wall, a wall strengthened with SRF sheet in conventional detail, and a wall strengthened with SRF sheet in the new detail, were tested to verify their seismic performances. These recent test results are reported here with an outline of past research on SRF columns.

2. SEISMIC EVALUATION AND RETROFIT IN JAPAN

Standardized practical effort of seismic retrofit for old reinforced concrete buildings in Japan has started from the middle of 1970',not only by the lessons to the 1968 Tokachi-oki and 1978 Miyagiken-oki earthquakes but also by the official prediction of high seismicity in Tokai region from past periodical events and long blank term promoted the systematic seismic evaluation and retrofit in the region, so-called Countermeasures for Tokai

Earthquake. In the first stage most of the evaluations were carried out on public buildings then moved to private buildings as well, but to a limited number of buildings, until the 1995 Kobe earthquake, which raised seriously the awareness of building owners.

On the other hand, the standard has been developed in mid 1970' and applied and sophisticated with research. The handbook, entitled Standard for Evaluation of Seismic Capacity of Existing RC Buildings, provides a method of expressing the seismic performance for existing reinforced concrete buildings through a continuous index and judges their seismic safety. The Standard for seismic evaluation in Japan is outlined in the following section.

3. SEISMIC PERFORMANCE INDEX

The Standard provides an approximated calculation method for the seismic performance of buildings in terms of two indexes, the seismic index of structural elements, Is, and the seismic index of nonstructural elements, IN. The Standard was developed for the purpose of evaluating a large number of buildings in the shortest possible time. Therefore, while referring to other already-proposed seismic design and evaluation methods, the method was simplified as much as possible without losing the essence, so that three levels of calculation methods are provided from simple to sophisticated one called as the first, second and third screening levels.

In the Standard, the seismic performance index of a building is expressed by the *Is*-Index for each story and each direction, as shown in Eq. (1):

$$I_S^{\bullet} = E_0 . S_D . T \tag{1}$$

where:

E_0 = Basic seismic index of structure (defined in 3.2).
S_D = Irregularity index (defined in 3.3).
T = Time index (defined in 3.4).

E_0 is a basic structural index calculated from strength index (C), ductility index (F), and story index (ϕ), C-Index denotes the lateral strength of the buildings in terms of shear force coefficient. F-Index denotes the ductility index of the building ranging from 0.8 (most brittle) to 3.2 (most ductile), depending on the sectional properties such as bar arrangement, member proportion, shear-to-flexural-strength ratio etc. ϕ is a modification factor to allow for the mode shape of the response along the building height. Basically in the Standard, a simple formula of $\phi = \frac{n+1}{n+i}$ is employed for the i-th story level of an n-storied building by assuming straight mode and uniform mass distribution.

S_D- and T-Index are reduction factors to allow for the disadvantages in the seismic performance of structures. S_D-Index, basically ranging from 0.4 to 1.0, is for modifying E_0-Index due to unbalanced distribution of stiffness both in the horizontal plane and along the height of the structure, resulting from irregularity and complexity of structural configuration. *T*-Index, ranging from 0.5 to 1.0, is employed to allow for the deterioration of strength and

ductility due to age after construction, fire and uneven settlement of foundation.

The first level procedure is the simplest but most conservative since only the sectional areas of columns and walls and concrete strength are considered to calculate the strength, and the inelastic deformability is neglected. The ductility index is simply assumed as 1.0 in a case without extremely brittle columns or 0.8 otherwise.

In the second and third level procedures, ultimate lateral load carrying capacity of vertical members or frames are evaluated using material and sectional properties together with reinforcing details based on the field inspections and structural drawings. The basic index E_0 is defined in the following ways:

Ductility-dominant basic seismic index of structure

$$E_0 = \frac{n+1}{n+i}\sqrt{E_1^2 + E_2^2 + E_3^2} \tag{2}$$

where:

$E_i = C_i \times F_i$

C_1 , C_2 , C_3 = The strength index C of the first, second and third group

F_1 , F_2 , F_3 = The ductility index F of the first, second and third group

$$E_0 = \frac{n+1}{n+i}\left(C_1 + \sum_j \alpha_j C_j \right).F_1 \tag{3}$$

where:

α_j = Effective strength factor in the *j*-th group elements at the ultimate deformation R_1 corresponding to the first group elements (ductility index of F_1)

The basic index of Eq. (2) and Eq. (3) denotes the earthquake intensity when the inter-story drift response would attain its limit state. The second screening considers only the vertical members, such as columns and walls, while the third screening considers beams as well. The methods or Eqs. for evaluating strength and deformability of the members are prescribed in the standard.

The elements are classified into three groups at the maximum for calculating ductility-dominant basic seismic index. First group is for brittle element, third group is for ductile element, and second group is medium. The ductility index as the boundary of groups can be chosen to make E_0 the biggest. Here, the ductility index of all group elements must be bigger than 1.0, and less than that in ultimate deformation of structure.

The load deformation relations in i-th story is calculated and idealized as shown in Fig. 1. The relations are idealized as a system consisting of three levels of ductility indices F_1, F_2 and F_3. The Eqs. (2) and (3) provide the earthquake intensities corresponding to the limit states at the ductility levels of F_3 and F1, respectively. Therefore, the basic index may generally be taken as either lager one of above two. The Eq. (2) gives higher values for systems mostly with ductile members, while the Eq. (3) gives higher values mostly for systems with non-ductile members.

However, to consider the value given by the Eq. (2), it should be confirmed that brittle failure of some columns would not induce partial collapse of the structure at a smaller deformability than F3 level, otherwise the structural limit state should be defined at the deformability that the partial collapse would occur, within which the index shall be calculated by Eq. (2). The method of calculating such deformation is also given in the Standard. The detailed calculation method for evaluating the ductility of partial collapse is clearly prescribed in the recent 2001 version. This is achieved by the judgment of the "second-class prime elements": in case a column could not carry the axial load beyond the ductility level, even by considering redistribution of the gravity axial load to the adjacent members, the column is judged as "the second-class prime element" and the associated deformation of partial collapse is defined as the limit state. The ductility index is defined as the deformation where the lateral resistance starts to decay. In the former version, the axial capacity of column beyond the defined ductility level is assumed to be zero, namely that the axial capacity is lost simultaneously with the shear failure before or after flexural yielding. However, the axial load capacity could be maintained beyond the defined ductility level. In the 2001 version, the residual axial load capacity beyond the defined ductility level may be account for the judgment of collapse. The calculation method for the residual axial capacity is given in the Standard. The members' capacities required for redistribution, such as the connecting beam strengths, shall be checked. The axial capacity of the adjacent members shall also be checked. If the axial load can be sustained by the residual capacity or adjacent elements, the column is not judged as not "the second-class prime element," but as "the third-class element," and the limit state may be taken as larger than the defined ductility level.

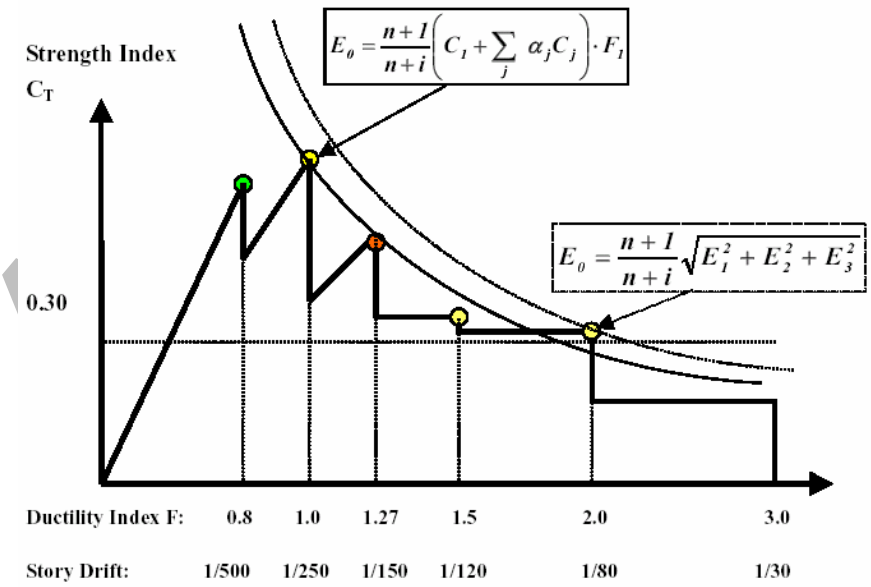

Figure 1. Idealized relations of lateral strength and ductility for seismic index

4. SEISMIC RETROFIT OF COLUMN USING POLYESTER SHEET

SRF (Super Retrofit with Flexibility) is a strengthening method of old reinforced concrete structures using flexible and ductile chemical fiber sheet such as polyester sheet. Past researches for verification of the method for the retrofit of non-ductile columns are outlined.

4.1 Static column test

Thirty-eight column specimens were tested in total in three years, from 2000 to 2002, and which are referred herein as first, second and third phase [Kabeyasawa et al, 2001 and 2002]. The horizontal section of the column specimens was 300mm×300mm and their height was 900mm. The hoops were designed according to the code of practice before or during the 1970's. The strengths of concrete were varied from 13.5MPa to 18MPa, so that the method may be applied to existing buildings of relatively low quality. Some of the specimens were subjected to constant axial loads and lateral force, while some others were tested under varying axial loads, which were controlled in proportion to the measured restoring shear force. The constant axial loads corresponded to the axial force ratio of about 0.2 or 0.3, while axial force ratios were varied from -0.15 in tension to +0.85 in compression, consequently.

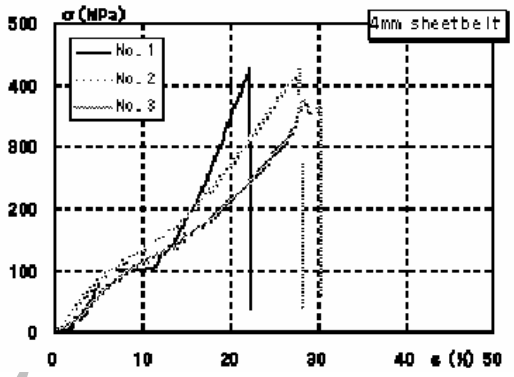

Figure 2. Tensile stress-strain relations of the polyester sheet

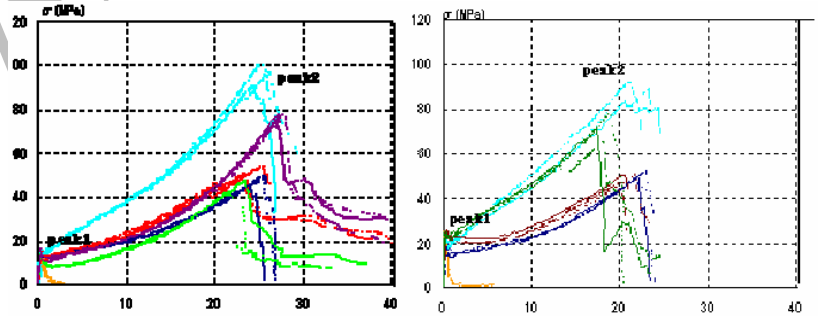

(a) Cylinder of fc=13.5Mpa (b) Cylinder of fc=18MPa

Figure 3. Stress-strain relations from axial test of cubes confined with the belt

Relatively thick and stiff belt-type polyester sheets was were used for strengthening from the second phase to improve not only axial capacity at large drift but also lateral shear resistance after shear cracking. The width and nominal thickness of the polyester belt are were, respectively, 64mm and 4mm. Obliquely winding bandage-type with single layer was used as the standard type of confinement. At the two ends, one layer was additionally wound as an anchorage. Only epoxy urethane adhesive was used to bond the belt to concrete and as to the anchorage. The nominal tensile strength of the belt was 484N/mm^2, whereas the strength from the tensile test was 412N/mm^2 for the actual thickness of 4.7mm at the strain of around 26%, as shown in Figure 2. This property with ductility to a great extent of over 20 percent strain is the strong advantageous point of the SRF method by which the column can be made super flexible, ductile and redundant.

Compression tests on prisms and cubes confined with the belt-type were also conducted, and the stress-strain relations of the cubes are shown in Figure 3. The results of the second phase were basically not much different from the cube tests of the first phase. However, the amount of confinement was relatively large in these cases because of the belt type, where the loss of strength after peak 1 was small and the peak 2 strengths rose up from to 40 to 90MPa, which were both much higher than the bare concrete strength. It is worth to note that the peak 2 strengths were almost same for both levels of concrete strength, and were mainly dominated by the amount of confinement.

(a) Specimen No. 12 (32.400rad) (b) Specimen No. 13 (48.400rad)

Photo 1. Typical failure modes of specimens with/without sheet

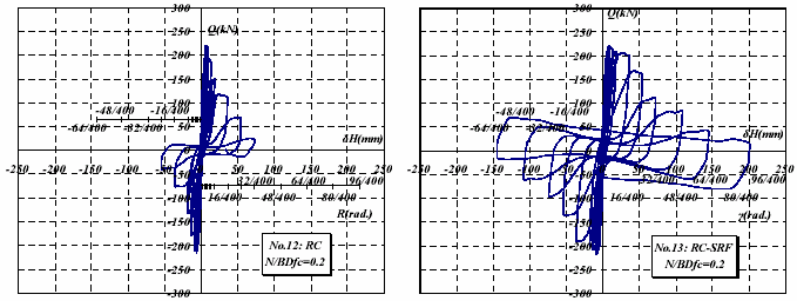

(a-1) No.12 (RC without sheet) (a-2) No.13 (RC with SRF sheet)

Figure 4. Hysteresis relations between shear force and lateral displacement (Phase 2, constant axial load N/BDfc=0.2, fc=18MPa)

In the first phase, the decay of lateral strengths in bare columns once observed after shear cracking of concrete, while the strength decay could be made gradual. The method using the multiplied thin SRF sheets is less effective and the SRF method with epoxy bond in addition slightly improved the behavior from bare specimens. After the seismic test to maximum drift of 24/100, some of the specimens were returned to the origin and axial compression test was conducted. The specimen could sustain more than axial load ratio of 1.0 (N=Acfc), which was limited by the capacity of vertical jacks.

In the second phase, with development of sheet belt-type reinforcing method from the first phase result, all specimens strengthened by SRF sheet is compared to their similar bared specimens. Typical failure modes, like those observed on specimens No.12 and No13 with a normal concrete strength of 18Mpa and undergoing constant axial load ratio of 0.20 are compared as shown in Photo 1. Also, while Specimen No. 12 failed in shear before yielding or another bare specimens failed in shear after yielding and lost the axial load carrying capacity under cyclic lateral load reversals within relatively low levels of story drift. Their similar SRF column specimens No. 13 with sheet failed in flexure and could sustain the axial load until the end of testing up to a drift of about 24/100 rad, which was, actually, the limit of the horizontal jack. The SRF method with the belt improved not only the axial load capacity but also maintained the lateral resistance after yielding. Typical hysteresis relations are compared in bare and SRF specimens, as shown in Figure 4(a) for No. 12 and Figure 4(b) for No. 13 under constant axial load ratio of 0.2. As to the axial deformations, the strengthening made them small enough, for example, less than 1mm (average strain of 0.001) at the story drift of 64/400 rad. in case of No.13.

4.2 Shaking table test

A shaking table test was conducted to verify the effectiveness of the new retrofit that would prevent the shear failure of columns and their axial collapse. The tested results showed the specimens with SRF retrofit survived tremendous dynamic load reversals and showed the structural safety of SRF and its ability to sustain the axial load and expand the ultimate state, [Kabeyasawa and Kim et al, 2002]. The specimens are two one-third-scale reinforced concrete wall-frame structures with considerable stiffness and strength eccentricity in the first story. The two specimens with the same sectional dimensions and reinforcement details, representing medium-rise reinforced concrete buildings with old details of column hoops, were constructed and tested simultaneously on the large shaking table at NIED, Tsukuba as shown in Photo 2. One specimen had bared reinforced concrete columns while the other had its columns strengthened with the SRF polyester sheet.

The RC columns failed to gravity load under the main input with maximum acceleration of 0.6G (Photo 3a). On the other hand, the SRF columns not only suffered slight damage under the same motion (Photo 3b), but also survived the succeeded three severe motions of still higher levels up to 0.8G with stable axial load capacity.

The hysteresis relations for columns of the RC specimen are presented in Figure 5 together with those of the SRF specimen.

The values of the maximum and minimum shear force and displacement for RC specimens are indicated in parentheses. The solid and dotted lines represent calculated shear strength (112.9kN) and shear at calculated flexural strength (125.5kN), respectively, for the

two RC columns. During the response to CHILE (50kine)-1st, the stiffness and strength degradations of the RC specimen became rapidly significant under reversed cyclic loadings and resulted in collapse when the elapsed time was around 20 sec. On the other hand, the hysteresis relations of the SRF specimen showed stable behavior without strength decay.

After removing the collapsed RC specimen from the shaking table, the strengthened specimen was subjected to the three base motions with higher levels, TAK125, CHI63 and CHI50-2. Maximum response and considerable residual deformations was generated after CHI63 and CHI50-2. Nevertheless, the SRF frame remained structurally stable as regard to the axial load although the decay in lateral stiffness and strength and the accumulation of axial deformation, the fact that SRF specimen survived three additional higher base motions, although permanent lateral and axial deformations were considerable, verified the effectiveness of SRF reinforcing method in this test.

Photo 2. Eccentric pilotis frames on the shaking table at NIED

(a) RC specimen (b) SRF specimen

Photo 3. Columns after CH150-1

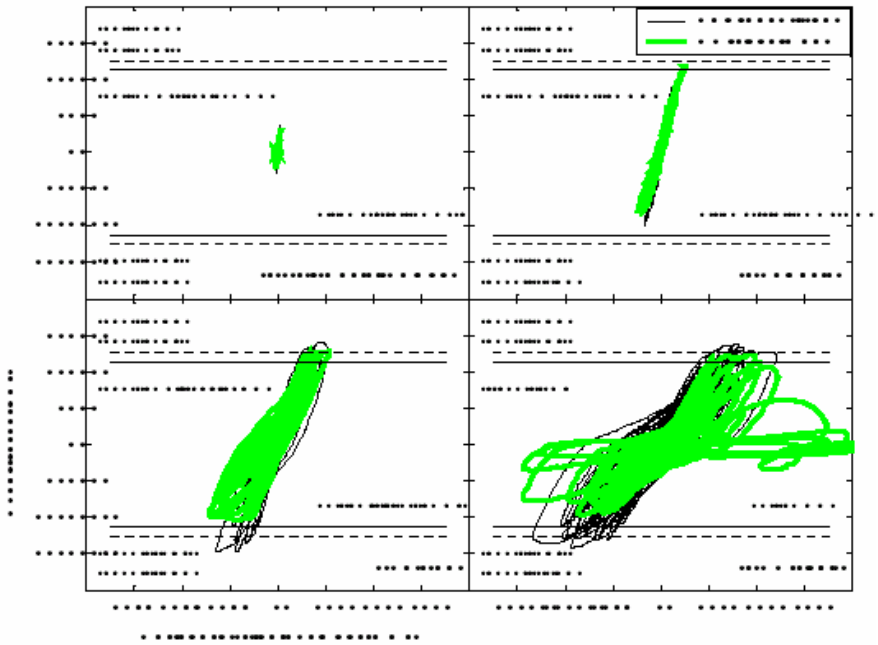

Figure 5. Shear force and displacement relation

5. WALLS STEREGTHED WITH POLYESTER SHEET

Static tests on wall members were planned and conducted in November 2004 to verify the effectiveness of SRF strengthening on walls, especially after the introduction of a new joint detail for the sheet strengthening.

5.1 Method of testing for walls

Tested specimens are three one-third scale reinforced concrete walls with boundary columns as listed in Table 1: (1) RC-M: the Proto-type bare wall that is constructed with details in accordance with Japanese old design specifications, as listed in Table 1(a) and shown in Figure 6. These details are common to the three specimens. (2) SRF-A: the specimen is strengthened after construction using SRF sheet, where the anchorage detail for the sheet at the inner edge of wall panel and boundary column is of a conventional type using L-shaped steel as shown Figure 7. (3) SRF-X: the specimen is strengthened after construction using SRF sheet with a new detail, where special ring-plate joint devices are used for the anchorage at the corner of the wall panel as shown in Figure 8 and Figure 9.

The sectional and reinforcement details of the bare reinforced concrete wall specimen are shown Figure 6. The reinforcement details follow the old code requirements in Japan before 1971. The column's hoop is of a D4 bar at the spacing of 100mm, which corresponds to D13 bar at the spacing of 300mm in the full scale. The wall reinforcement ratio is 0.0025, which is equal to the minimum requirement before 1970 and also at present. The nominal strength of concrete is 24MPa.

Material properties of concrete and steel were to be basically common to the three specimens as listed in Table 2(a) and (b). However, the concrete strength at the time of testing RC-M was a little less than the nominal value, while it was almost equal to the nominal value when SRF-A and SRF-X were tested. The property of SRF sheet is given in Table 2(c).

The conventional detail for strengthening the specimen SRF-A is shown in Figure 7. The sheet belt is wound horizontally around the section and attached with the urethane adhesive bond for SRF. Then the holes are perforated at the spacing of 190mm through the wall panel along the inner edges adjacent to the boundary columns. The sheet was constrained and anchored by mean of the L-shaped steel and the high strength bolts of 10mm at the inner edge. This detail is to be effective not only for the increase of the shear resistance of the wall in the in-plane direction but also for the transverse direction. The detail is necessary because the strengthening of the boundary columns is also required for the transverse loading in most cases of retrofit design of a whole structure.

The new detail for SRF-X is shown in Figure 8. Four special steel ring-plate joint devices shown in Figure 9 are developed and placed at the four corners of the wall panel. The concrete of the corners is removed and the gap with the joint was filled in with mortar. The height of the joint is selected equal to the column's depth of 250mm. The sheet belts are wound horizontally around the column and the wall panel at the bottom and top and also diagonally on the wall panel through the joint devices. The remained medium wall panel is strengthened as in the conventional detail with the sheet belt and L-shaped steel.

The loading system built in the testing laboratory of ERI is shown in Figure 10. Oil jack in the horizontal direction and two oil jacks in the vertical direction were controlled to apply a constant vertical load and a lateral force with a constant moment-to-shear ratio. The constant axial load N was 450kN which corresponds to the gross load of the boundary columns 2Ac, namely as N/(2Acfc)= would come to 24MPa. The lateral shear is applied with lateral jack through the steel beam attached above the top beam stub of the specimen. The bending moment is applied by the two vertical jacks in proportion to the lateral shear in a way the moment – to – shear ratio at the wall base is kept constant as M/QLw=1.0, where Lw is the effective wall depth. Lw =16000mm. Pantographs were attached to the top steel beam and the ceiling floor to restrain accidental out-of plane deformation. The three jacks, equipped with load cells, have the capacities of 1000kN in tensile and compressive loading and 400mm stroke with the universal joint clevises at their two ends.

Table 1. List of wall specimens
(a) Sections and reinforcement common in three specimens

Element	Section	Height	Main bars	Hoop/Web/Stirrup
Column	250x250	1400	16-D 10 (pg=0.018)	2-D4@100 (pw=0.0010)
Wall panel	80x1550	1400	20D4@130 (pw=0.0025)	2-D4@130 (pw=0.0025)
Beam	400x600	400	8-D19	4-D10@100

(b) Strengthening method

Name	Strengthening for column	Strengthening for wall panel	Anchorage
RC-M	None	None	
SRF-A	1 layer	1 layer	L-steel
SRF-X	1 layer (2 layers*)	1 layer + 2 layers**	Ring-plate joint device + L-steel

*** top and bottom ends (h=250mm)**
**** X-type bracing**

Table 2. Material properties

(a) Concrete

Name	Nominal Strength (N/mm^2)	Elastic Young Modulus (N/mm^2)	Measured Strength (N/mm^2)	Strain at strength
RC-M	24	2.47	22.4	0.00159
SRF-A	24	2.50	24.36	0.00172
SRF-X	24	2.49	24.38	0.00168

(b) Steel

Mark	Nominal Strength (N/mm^2)	Elastic Young Modulus (N/mm^2)	Yield Strength (N/mm^2)	Yield Strain	Maximum Strength (N/mm^2)
D4	SD295	1.59 10^5	339.8	0.00414	560.2
D10	SD345	1.72 10^5	397.8	0.00244	557.0

(c) Sheet

Name	Thickness (mm)	Width (mm)	Nominal Strength (N/mm)	Nominal Elongation Strain	Measured Strength (N/mm)	Measured Elongation Strain
SRF-450	4.0	45	400	0.1	520	0.129
SRF-2100	2.0	100	400	0.1	421	0.125

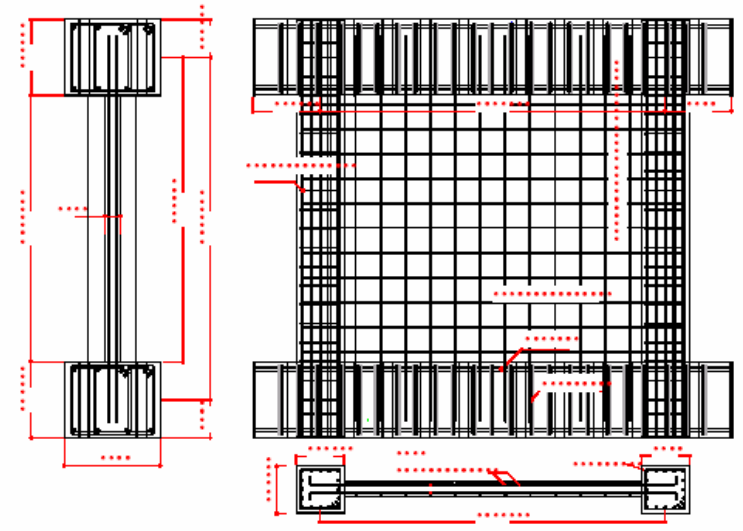

Figure 6. Reinforcement details of bare wall specimen

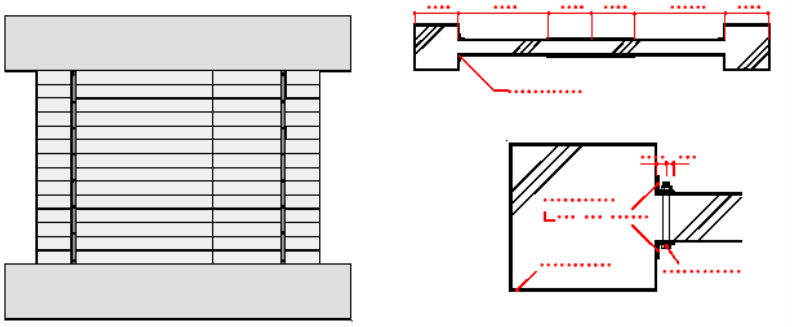

Figure 7. Conventional detail for SRF sheet strengthening

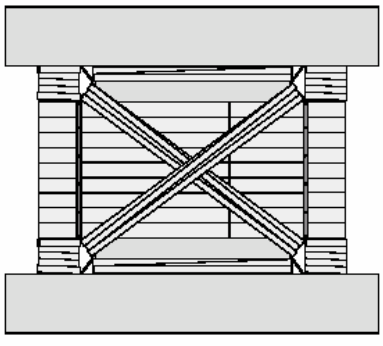

Figure 8. New detail for SRF sheet strengthening

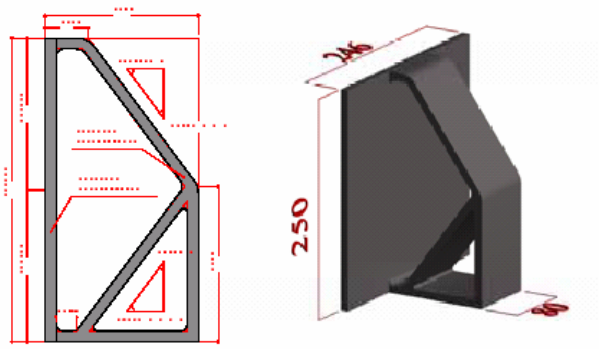

Figure 9. Ring-plate joint device for SRF

The shear strength of the bare reinforced concrete specimens, which was calculated using the design Eqs. in practice in Japan, was about 0.8 of the shear at the ultimate flexural strength. Therefore the shear failure was expected to occur prior to the attainment of the ultimate flexural strength. On the other hand, ductile behavior was expected, to some extent, by the increase of the shear resistance for the specimens strengthened by sheet.

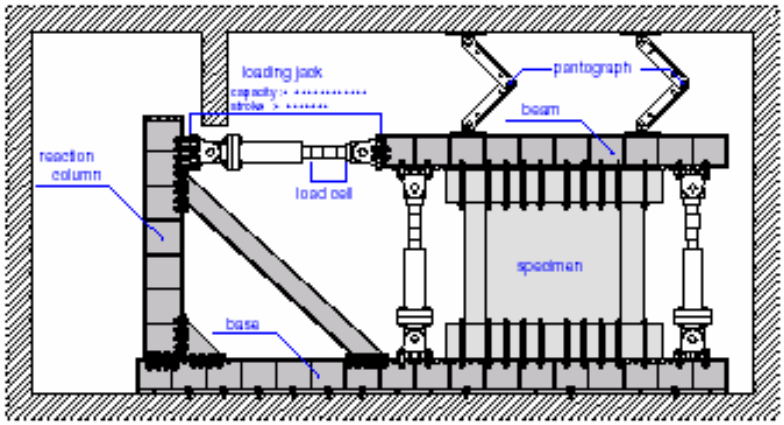

Figure 10. Loading setup

5.2 Wall test results failure modes of walls

The ultimate failure modes of the three specimens after the tests are shown in photo 4. The lateral displacement was measured at the bottom of the beams, at a height of 1400mm from the wall base. The processes of failure are outlined as well as the capacities in terms of the lateral and vertical loadings.

The bare wall specimen RC-M failed in shear at the deformation angle of about 1/200. The shear cracking in the wall panel widened and diagonal shear tension failure occurred through the boundary columns. The lateral load resistance was lost simultaneously with the axial capacity at the shear failure. The lateral deformation proceeded over 1/50radian, because the resistance of the wall dropped suddenly.

The specimen SRF-A strengthened with the conventional detail failed in shear at the deformation angle of 1/100rad. The deformation angle of the shear failure could be enlarged probably because the sheet was effective to increase the shear resistance and the associated deformation. The lateral resistance fell down steeply after the failure to half of the peak value and the lateral displacement proceeded up to 1/33rad as in the case of the bare wall RC-M. The constant axial load capacity could be maintained, up to the loading level of 1/33rad, however, because the steel plate at the corner and the fastening bolt seemed to be nearly broken during the 1/33rad, the loading and the lateral resistance could not be recovered after the shear failure and the test was terminated.

The specimen SRF-X strengthened with the new detail using the joint devices and the diagonal sheet attained the maximum strength at the deformation angle of 1/75rad. The lateral resistance decayed gradually after the peak strength by which the displacements for

cyclic reversal could be controlled as scheduled. Although the gradual progress of sliding shear failure and crushing was observed at the lower panel where the sheet was not provided, relatively stable behavior was observed under cyclic loading up to 1/15rad. The lateral resistance of more than half of the peak strength was maintained and then recovered in larger drift as was observed in SRF columns. The devices deformed and partially broke at the connected edges during cyclic loading of large amplitudes but did not cause fatal unstable behavior. The axial load was also maintained stable until the end of testing.

6. COMPARISON OF ULTIMATE STRENGTHS

The maximum strengths observed in the test are compared with the calculated ultimate strengths as shown in Table 3. The flexural strength is calculated from the approximate design Eq. based on the flexural theory. The shear strengths are calculated from the design Eq. (4) in AIJ guidelines (1999, 5) based on arch and truss mechanism and the design Eq. (5) for minimum values PA standard (2001, 1) and BCJ bA arch and truss shear resistance of shear strength in JBDE guidelines (2000, 6):

$$Q_{SU1} = t_w.l_{wb}.(p_z + p_{f1}.\sigma_{f1}).\cot\phi + \tan\phi.(1-\beta).t_w.l_{w\alpha}.v.\sigma_{f1}/2 + Q_{ZNFX} \quad (4)$$

$$Q_{SU2} = \left[\frac{0.053p_{tx}^{0.23}.(\sigma_B + 18)}{MI(Q./) + 0.12} + 0.85\sqrt{p_s.\sigma_{sy} + p_{f1}.\sigma_{f1}} + 0.1\sigma_\alpha\right].t_\alpha.j + Q_{XRFX} \quad (N) \quad (5)$$

Table 3. Calculated and observed strengths of the wall specimens (unit in kN)

Specimen	Observed	Flexural Q_{fu}	Shear [AIJ, 5] Q_{SU1}	Shear [BCJ, 6] Q_{SU2}
RC-M	721	779	631	621
SRF-A	818	779	727* (812)**	610* (663)**
SRF-X	817	779	820* (973)**	756* (968)**

Horizontal and diagonal sheet strains: *.0025 and 0.005, measured and averaged for total length, ** 0.005 and 0.01, twice as measured.

Q_{SU1}, Q_{SU2}: calculated shear strength, p_s, σ_s: ratio and yield strength of web reinforcement in wall panel, p_{f1}, σ_{f1}: equivalent ratio and stress of the horizontal sheet, Q_{XRFX}: shear carried by the tensile diagonal sheet, calculated as $Q_{SRFX} - A_f\ \sigma_{f2}\cos\theta$, A_f: area of the diagonal sheet, θ: angle of diagonal sheet, σ_{f1}, σ_{f2}: effective strains in the horizontal and diagonal sheet at failure (σ_{f1}-$E_f\,\varepsilon_{f1}$, σ_{f2}-$E_f\,\varepsilon_{f2}$), ε_{f1}, ε_{f2}: effective strains in the horizontal and diagonal sheet at failure determined from measured in the test, E_f: elastic modulus of sheet.

The shear strength of SRF-A is calculated by the design Eqs. regarding the horizontal sheet as additional equivalent web reinforcement. That of SRF-X is calculated in the same way for

the horizontal sheet, to which the resistance of the diagonal sheet is added as above.

The shear strengths of SRF-A and SRF-X are calculated considering the effect of the sheet from the measured strains by two ways: (1) ε_{f1}-0.0025 for horizontal direction and ε_{f2}-0.005 for diagonal direction, and (2) twice of these, namely, ε_{f1}-0.005 and ε_{f2}-0.01. The former assumption (1) is based on the averaged strains measured at the shear failure in the tests for the overall length, which would be the most conservative for the effect of the sheet, namely, the fact of neglecting the bond effect between the sheet and the concrete. The latter assumption (2) is based on the past research on columns reflecting the effect of bond on the resistance, namely, simulating strain concentration nearby the cracks.

The observed maximum strength of 721kN of RC-M was less than the calculated flexural strength of 779kN and higher than the calculated shear of 621kN or 631kN. The reinforced concrete specimen RC-M failed in shear after flexural yielding and before attainment of flexural ultimate state during the test, which the calculation, though both Eqs. for shear are slightly conservative. On the other hand, the observed maximum strengths of 818kN for SRF-A and 817KN for SRF-X, attained the flexural ultimate and exceeded the calculated flexural strength. Therefore, the potential shear strengths could be made higher than the flexural strengths so that the flexural failure would precede the shear failure and the deformability could be increased by the SRF strengthening. The specimen SRF-X, particularly, showed stable behavior under cyclic loading up to 1/15rad.

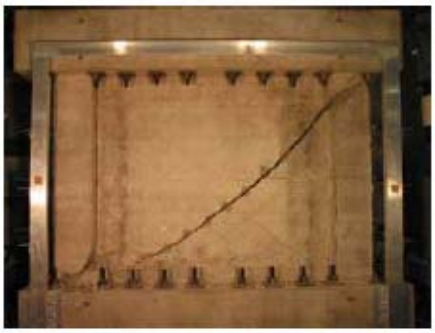

(a) RC-M: Bare reinforced concrete

(b) SRF-A: Strengthened with conventional detail

(c) SRF-X: Strengthened in the new detail

Photo 4. Failure modes at limit deformation

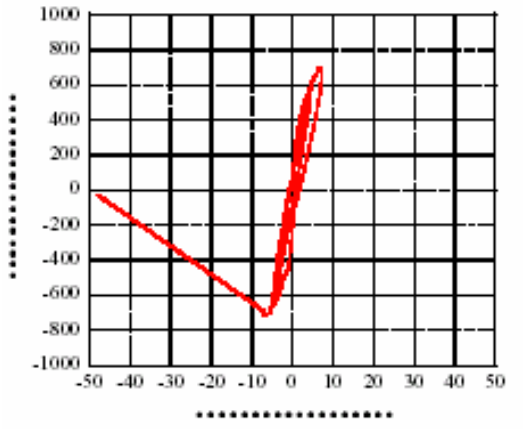

(a) RC-M: Bare reinforced concrete

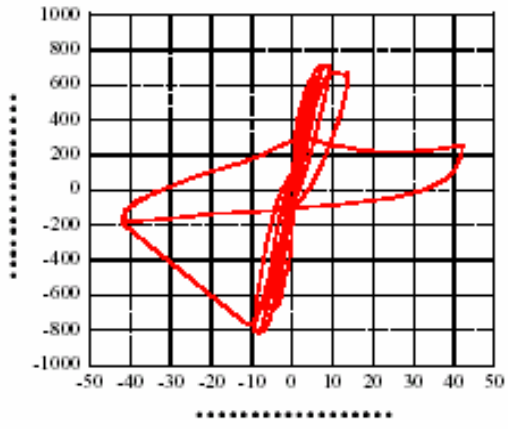

(b) SRF-A: Strengthened in conventional detail

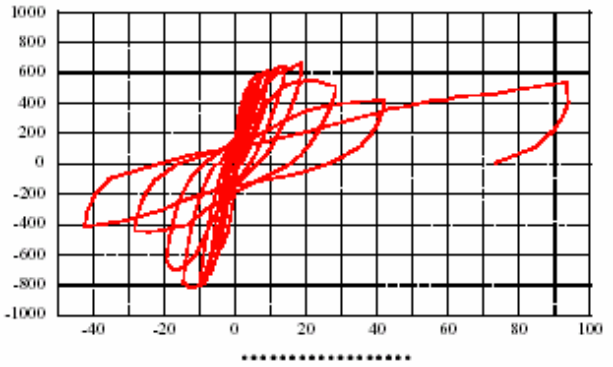

(c) SRF-X: Strengthened in the new detail

Figure 11. Hysteresis relations

6.1 Evaluation of wall deformability

The effects of the sheet on the deformability are discussed with the current evaluation methods in practice. Evaluation methods for ultimate deformability are given in the AIJ guidelines (1999, 5) and also in the JBDPA standard (2001, 6), which are based on the margin of shear strength to the shear induced at flexural ultimate. The effective stresses or strains also in the sheet are assumed as in two ways as above for the shear strength estimation, namely (1) ε_{f1}-0.0025 for horizontal direction and ε_{f2}-0.005 for diagonal direction and (2) twice of these, namely, ε_{f1}-0.005, ε_{f2}-0.01. In the AIJ guidelines, the ultimate deformation angle R_u is assured in design of hinging region of the flexural walls by making the shear strength $Q_{SU1}(v)$ higher than the shear at flexural strength Q_{fu}, and $Q_{SU1}(v)$ is to be calculated from the design Eq. (4) using the effective factor of concrete v reduced by the following Eq. (6) as:

$$
\begin{aligned}
&v = v_0 && R_u < 0.005 \\
&v = (1.2 - 40R_u)v_0 && 0.005 \le R_u < 0.002 \\
&v = 0.4v_0 && 0.02 \le R_u
\end{aligned} \qquad (6)
$$

$$v_0 = 0.7 - \frac{\sigma_B}{2000} : \text{effective factor for non - hinge region}$$

$$\sigma_B : \text{concrete strength in } (\text{N/mm}^2)$$

Therefore, if the effective factor v is calculated to satisfy $Q_{SU1}(v)=Q_{fu}$ for the wall specimens and the observed deformation capacities in the test are compared with above Eq. (6), then the evaluation method in the guidelines can be verified. As plotted in Figure 12(a), the observed deformation capacities of the SRF specimens are generally higher than the Eq. (6). The both assumptions on the effectiveness of the sheet, or on the strains, may be appropriate for the evaluation method in AIJ guidelines for deformability.

In the JBDPA seismic Evaluation Standard, the deformability of the wall members are evaluated as the ductility index F using the shear strength $Q_{av}(-Q_{SU2})$ calculated by the Eq. (5) and the shear at flexural strength Q_{fu} as follows:

$$
\begin{aligned}
&Q_{av}/Q_{fu} \le 1.0 && F = 1.0 \quad (R_u = 0.004) \\
&1.0 < Q_{av}/Q_{fu} && \text{interpolation} \\
&Q_{av}/Q_{fu} \ge 1.3 && F = 2.0 \quad (R_u = 0.0125)
\end{aligned} \qquad (7)
$$

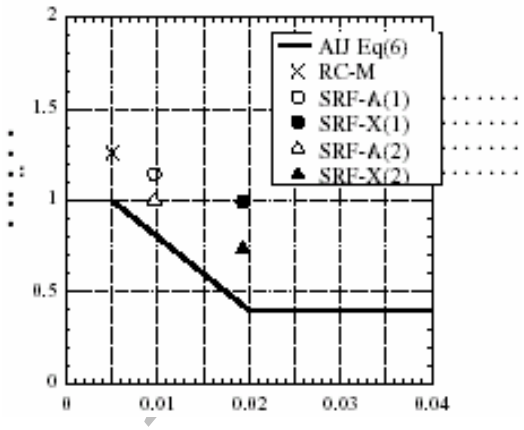

Ultimate deformation angle (rad.)
(a) AIJ Guidelines

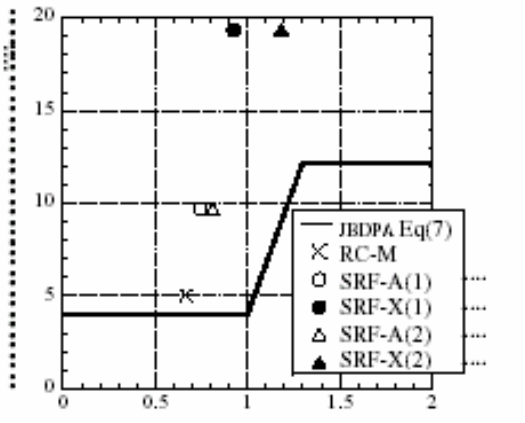

Shear strength margin: Q_{su}/Q_{fu}
(b) JBDPA Standard

Figure 12. Observed and calculated ultimate deformability of reinforced concrete walls and SRF walls

The observed deformation capacities of the wall specimens are also compared with Eq. (7) as shown in Figure 12(b). The observed deformation capacities of the SRF specimens are

also generally higher than those given by Eq. (7). The assumptions on the effectiveness of the sheet may be appropriate also for the evaluation method of the deformability in the Seismic Evaluation Standard as well.

It may be concluded that SRF using polyester sheet is effective for the increase of deformability, which is especially much more effective with the new detail, and can be estimated by the current design Eqs. in practice.

7. CONCLUSIONS

The recent edition of the seismic evaluation standard for existing reinforced concrete buildings in Japan was introduced. The Standard has long been used in practice but the new edition was translated into English recently. A method of evaluating the limit state deformation of a partial collapse due to the loss of axial load carrying capacity of a column is outlined

As an example of recent development on retrofit techniques in Japan, an economical and efficient method for strengthening brittle columns is introduced. SRF, super retrofit with flexibility, using flexible fiber sheet such as polyester sheet belt, has been verified to be effective and in practical use for the retrofit of reinforced concrete columns. SRF was applied to the retrofit of walls, for which three retrofit concrete wall specimens were tested. The bare wall specimen failed in shear at the deformation angle of 1/200 rad. when the lateral resistance and the gravity load carrying capacities were lose simultaneously, however, the wall specimens strengthened by the SDF sheet attained higher shear strengths and ultimate deformabilities. The SRF wall with a conventional detail of anchorage failed in shear at 1/100 rad, and the lateral resistance fell down after the failure, though the axial load capacity was maintained during loading up to 1/33 rad. The SRF wall with specially developed joint devices and diagonal sheets attained higher deformability. A sliding failure occurred at 1/75 rad. by which the lateral resistance decayed gradually, though much more stable behavior was observed up to 1/15 rad, maintaining both lateral and axial capacity. It maybe concluded that SRF can also be applied to the retrofit of reinforced concrete walls and the new detail is much more effective for the increase of deformability. The deformation capacities of the SRF walls observed in the test are generally higher than estimations using the current evaluation methods both in the seismic evaluation standard and the displacement-based design guidelines, which may be used for retrofit design.

Acknowledgements: The seismic evaluation standard based on the English version (JPBDA, 2005), for which the author is one of the editors. The static column tests were conducted in the Structural Testing Laboratory at Yokohama University, with Dr. Akira Tasai, YNU and Dr. Shunichi Igarachi, Square Inc. The test of frame was conducted at the Shaking Table, NIED, Tsukuba with Dr. Kim, Y-R. Nobuyuki Ogawa, NIED and Dr. Shunichi Igarachi.

The static wall test was conducted in Structural Testing Laboratory at ERI, with Dr. Yasushi Sanada, ERI. The cooperative studies in the tests and data analyses of the former students, at ERI or YNU, Mr. Hiroshi Koizumi, Ms. Yasuko Ohsugi, Mr. Hassane Ousalem,

Kengo Kamano, Mr. Daichi Tanabe and Mr. Rei Tamura, Mr. Maski Murase are gratefully acknowledged. The strengthening method introduced herein has been an international patent pending as "SRF" method by Square Inc., Japan.

REFERENCES

1. JBDP, Standard for Evaluation of Seismic Capacity of Existing RC Buildings, The Japan Building Disaster Prevention Association, 2001.
2. Kabeyasawa, T., Tasai, A., Igarashi, S., A New Method of Strengthening Reinforced Concrete Columns Collapse against Axial Load Collapse during Major Earthquake, Proceedings of the Third Workshop on Performance-based Engineering on Reinforced Concrete Building Structures, 2001, pp. 371-384.
3. Kabeyasawa, T., Tasai, A., Igarashi, S., An Economical and Efficient Method of Preventing Old Reinforced Concrete Buildings from Collapse under Major Earthquake, Proceedings of 7NCEE, CD-ROM, Boston, 2002.
4. Kabeyasawa, T., Igarashi, S., Kim, Y-S., Shaking table test of reinforced concrete frames for verification of seismic strengthening with polyester sheet, 13th World verification of seismic strengthening with polyester sheet, Proceedings Conference on Earthquake Engineering, Vancouver, B.C., Canada, Paper No. 402, August 1- 6, 2004
5. AIJ, Design Guidelines for Earthquake-Resistant Reinforced Concrete Buildings Based on Inelastic Displacement Concept (in Japanese), Architectural Institute of Japan, 400pp., 1999.
6. BCJ, Design Guidelines for Structural Calculation (in Japanese), Building Center of Japan, 2000.